

Characterization of the Sterically Encumbered Terphenyl-Substituted Species 2,6-Trip₂H₃C₆Sn–Sn(Me)₂C₆H₃-2,6-Trip₂, an Unsymmetric, Group 14 Element, Methylmethylene, Valence Isomer of an Alkene, Its Related Lithium Derivative 2,6-Trip₂H₃C₆(Me)₂Sn–Sn(Li)(Me)C₆H₃-2,6-Trip₂, and the Monomer Sn(*t*-Bu)C₆H₃-2,6-Trip₂ (Trip = C₆H₂-2,4,6-*i*-Pr₃)

Barrett E. Eichler and Philip P. Power*

Department of Chemistry, University of California, Davis, One Shields Avenue, Davis, California 95616

Received May 12, 2000

The reaction of the recently reported sterically encumbered terphenyl tin(II) halide species Sn(Cl)C₆H₃-2,6-Trip₂ (Trip = C₆H₂-2,4,6-*i*-Pr₃), **1**, with 1 equiv of MeLi or MeMgBr afforded 2,6-Trip₂H₃C₆Sn–Sn(Me)₂C₆H₃-2,6-Trip₂, **2**, which is the first stable group 14 element methylmethylene (i.e., CH₃CH) analogue of ethylene (H₂CCH₂). Reaction of **1** with 1.5 equiv of MeLi yielded the stannylstannate species 2,6-Trip₂H₃C₆(Me)₂Sn–Sn(Li)(Me)-C₆H₃-2,6-Trip₂, **3**, whereas reaction of **1** with 1 equiv of *t*-BuLi gave the heteroleptic stannanediyl monomer Sn(*t*-Bu)C₆H₃-2,6-Trip₂ (**4**). The compounds **2–4** were characterized by ¹H, ¹³C (⁷Li, **3** only), and ¹¹⁹Sn NMR spectroscopy in solution and by UV–vis spectroscopy. The X-ray crystal structures of **2–4** were also determined. The formation of the stannylstannanediyl **2** instead of the expected symmetrical, valence isomer “distannene” form {Sn(Me)C₆H₃-2,6-Trip₂}₂, **6**, is explained through the ready formation of LiSn(Me)₂C₆H₃-2,6-Trip₂, **5**, which reacts rapidly with **1** to produce **2** which can then react with a further equivalent of MeLi to give **3**. The stability of singly bonded **2** in relation to the formally doubly bonded **6** was rationalized on the basis of the difference in the strength of their tin–tin bonds. In contrast to the methyl derivatives, the reaction of **1** with *t*-BuLi proceeded smoothly to give the monomeric compound **4**. Apparently, the formation of a *t*-Bu analogue of **5** was prevented by the more crowding *t*-Bu group. Compound **2** is also the first example of a stable molecule with bonding between a two-coordinate, bivalent tin and four-coordinate tetravalent tin. Both compounds **2** and **3** display large *J* ¹¹⁹Sn–¹¹⁹Sn couplings between their tin nuclei and the tin–tin bond lengths in **2** (2.8909(2) Å) and **3** (2.8508(4) Å) are relatively normal despite the presence of the sterically crowding terphenyl substituents.

Introduction

Recent studies of the reactivity of Pb(Br)C₆H₃-2,6-Trip₂ (Trip = C₆H₂-2,4,6-*i*-Pr₃) with MeMgBr, Li(*t*-Bu), and LiPh showed that the first two-coordinate lead(II) derivatives of simple organic ligands such as CH₃, *t*-Bu, or Ph could be stabilized by the use of the sterically encumbering terphenyl group C₆H₃-2,6-Trip₂ as coligand.¹ It was expected that the corresponding reactions of the related tin halide Sn(Cl)C₆H₃-2,6-Trip₂ (**1**)² with these reagents would lead to products with similar stoichiometries in which tin is bound to these simple groups. In general, stable, two-coordinate dialkyls or diaryls of tin(II) can be synthesized by the reaction of an Sn(II) halide with lithium alkyls or aryls, and, provided that the ligands are of sufficient size, the diorganotin(II) products are isolated either as monomers³ or as “distannene” dimers⁴ that feature tin–tin bonds with varying degrees of multiple character. With less crowded organic

ligands, for example, a Trip or a phenyl group, oligomers such as the three- or six-membered ring compounds *c*-{SnTrip₂}₃⁵ or *c*-(SnPh₂)₆⁶ are obtained. All of these species are related in that they feature two organic groups at each tin and have the metal in the formal oxidation state +2. Unlike these findings, it is now shown that the reaction between MeLi or MeMgBr with Sn(Cl)C₆H₃-2,6-Trip₂ does not lead to the isolation of the expected alkene-like symmetric product {Sn(Me)C₆H₃-2,6-Trip₂}₂ (**6**) but to the first instance of a stable group 14 element valence isomer of an alkene 2,6-Trip₂H₃C₆Sn–Sn(Me)₂C₆H₃-2,6-Trip₂, **2**, and the lithium salt 2,6-Trip₂H₃C₆(Me)₂Sn–Sn(Li)C₆H₃-2,6-Trip₂, **3** (Scheme 1), in which the tin atoms have different substituents and different formal oxidation states. In contrast, the reaction with *t*-BuLi gives the monomeric stannanediyl Sn(*t*-Bu)C₆H₃-2,6-Trip₂. The reasons for this unexpected result involve the unique steric properties of the bulky terphenyl group, the small size of the methyl substituents, and the relative weakness of the putative multiple Sn–Sn bond in **6**.

(1) Pu, L.; Twamley, B.; Power, P. P. *Organometallics* **2000**, *19*, 2471.

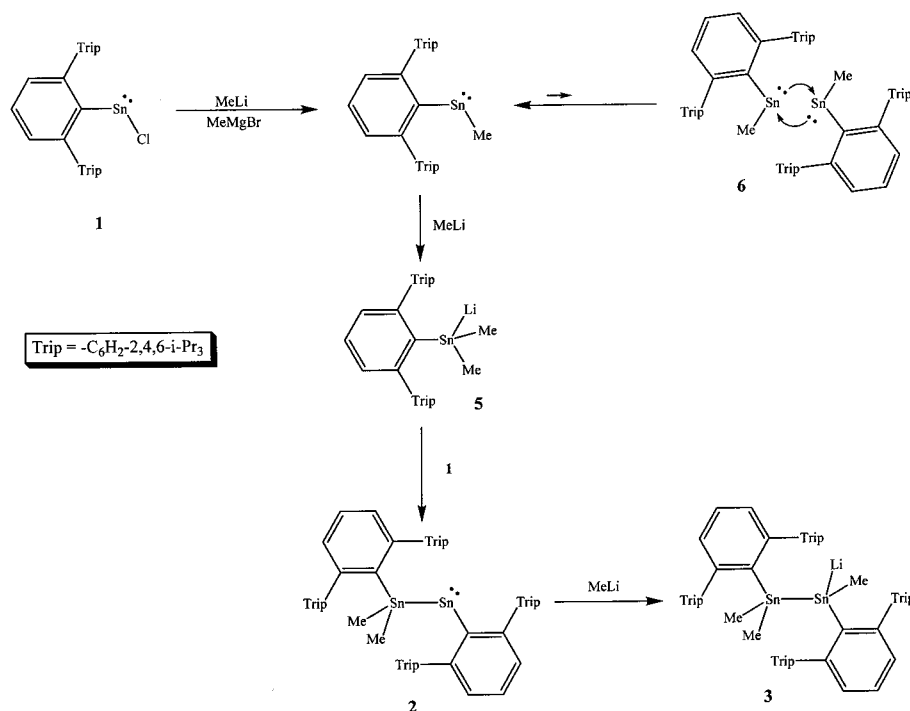
(2) Pu, L.; Senge, M. O.; Olmstead, M. M.; Power, P. P. *J. Am. Chem. Soc.* **1998**, *120*, 12682.

(3) For example: (a) Kira, M.; Yauchibara, R.; Hirano, R.; Kabuto, C.; Sakurai, H. *J. Am. Chem. Soc.* **1991**, *113*, 7785. (b) Weidenbruch, M.; Schlaefke, J.; Schäfer, A.; Peters, K.; Schnering, H. G. v.; Marsmann, H. *Angew. Chem., Int. Ed. Engl.* **1994**, *33*, 1846. (c) Simons, R. S.; Pu, L.; Olmstead, M. M.; Power, P. P. *Organometallics* **1997**, *16*, 1920. (d) Eaborn, C.; Hill, M. S.; Hitchcock, P. B.; Patel, D.; Smith, J. D.; Zhang, S. *Organometallics* **2000**, *19*, 49.

(4) For example: (a) Davidson, P. J.; Lappert, M. F. *J. Chem. Soc. Chem. Commun.* **1973**, 317. (b) Goldberg, D. E.; Harris, D. H.; Lappert, M. F.; Thomas, K. M. *J. Chem. Soc. Chem. Commun.* **1976**, 261. (c) Layh, U.; Pritzkow, H.; Grützmacher, H. *J. Chem. Soc. Chem. Commun.* **1992**, 260. (d) Weidenbruch, M.; Kilian, H.; Peters, H.; Schnering, H. G. v.; Marsmann, H. *Chem. Ber.* **1995**, *128*, 983.

(5) Masamune, S.; Sita, L. R. *J. Am. Chem. Soc.* **1985**, *107*, 6390.

(6) Olson, D. H.; Rundle, R. E. *Inorg. Chem.* **1963**, *2*, 1310.

Scheme 1. Illustration of the Possible Relationships between the Compounds **1–3**, **5**, and **6**

Experimental Section

General Procedures. All manipulations were carried out by using modified Schlenk techniques under an atmosphere of N₂ or in a Vacuum Atmospheres HE-43 drybox. All solvents were distilled from Na/K alloy and degassed three times before use. The compound Sn(Cl)C₆H₃-2,6-Trip₂ (**1**) was prepared according to literature procedures.² Solutions of MeLi, MeMgBr, and *t*-BuLi were purchased commercially and used as received. ¹H, ⁷Li, ¹³C, and ¹¹⁹Sn NMR spectroscopic data were recorded on a Varian INOVA 400 MHz spectrometer. ¹H and ¹³C spectra were referenced to the deuterated solvent. The ⁷Li spectrum of **3** was referenced externally to LiCl/D₂O and the ¹¹⁹Sn spectra were referenced externally to SnMe₄/C₆D₆. UV–vis data were recorded on a Hitachi-1200 spectrometer.

2,6-Trip₂H₃C₆Sn–Sn(Me)₂C₆H₃-2,6-Trip₂ (2**).** Method A: MeMgBr (0.77 mL, 2.30 mmol, 1.0 equiv) was added dropwise to a pale yellow solution of **1** (1.47 g, 2.31 mmol) in pentane (80 mL) at ca. –78 °C. Slow warming to ca. 0 °C caused the solution to turn bright green with a concomitant formation of a colorless precipitate (magnesium halide). The solution was further stirred at ca. 25 °C for 1 h and the solvents were removed under reduced pressure. The green solid was extracted with hexanes (100 mL) and the solution was filtered through a Celite pad. The volume of the solution was then reduced to ca. 10 mL and the flask was stored in a ca. –20 °C freezer overnight to afford green crystals of **2** (1.25 g, 0.98 mmol, 85%).

Method B: MeLi (1.45 mL, 2.32 mmol, 1.1 equiv) was added dropwise to a pale yellow solution of **1** (1.34 g, 2.11 mmol) in hexanes (60 mL) at –78 °C, to afford a bright green solution. The solution was stirred at –78 °C for 30 min and was allowed to warm to ca. 25 °C. A workup procedure similar to method A afforded green crystals of **2** (0.25 g, 0.20 mmol, 9%). Mp = 210–213 °C (dec to red). Anal. Calcd for C₃₇H₅₂Sn: C, 72.20; H, 8.52. Found: C, 72.88; H, 8.96. UV–vis (hexanes) λ_{max}, ε (mol^{–1} cm^{–1}): 689 nm, 271. ¹H NMR (C₆D₆, 399.77 MHz, 25 °C): δ –0.34 (s, 6H, Sn(CH₃)₂), 1.07 (br d, 24 H, ³J = 6.6 Hz, *o*-CH(CH₃)₂), 1.31 (d, 12 H, ³J = 7.0 Hz, *p*-CH(CH₃)₂), 2.85 (sept, 2 H, ³J = 7.0 Hz, *p*-CH(CH₃)₂), 2.99 (br s, 2H, *o*-CH(CH₃)₂), 3.21 (br s, 2 H, *o*-CH(CH₃)₂), 7.10 (s, 4 H, *m*-Trip), 7.07–7.22 (br m, 3 H, *p*- and *m*-C₆H₃). ¹³C {¹H} NMR (C₆D₆, 100.53 MHz): δ 0.34 (Sn(CH₃)₂), 24.12 (*o*-CH(CH₃)₂), 26.22 (*p*-CH(CH₃)₂), 30.85 (*o*-CH(CH₃)₂), 34.59 (*p*-CH(CH₃)₂), 121.90(*m*-Trip), 126.10 (*m*-Trip), 127.70 (*i*-Trip) 131.11 (br, *o*-Trip), 146.45 (*p*-Trip), 146.94 (*o*-C₆H₃), 147.19 (*m*-C₆H₃), 148.58 (*p*-C₆H₃), 165.23 (*i*-C₆H₃). ¹¹⁹Sn {¹H} NMR (C₆D₆, 149.24 MHz): δ

257.4 (Sn (four-coordinate), ¹J(¹¹⁹Sn–^{119/117}Sn) = 8332 Hz), 2856.9 (Sn (two-coordinate), ¹J(¹¹⁹Sn–^{119/117}Sn) = 8332 Hz).

2,6-Trip₂H₃C₆(Me)₂Sn–Sn(Li)(Me)(C₆H₃-2,6-Trip₂ (3**).** MeLi (2.40 mL, 3.84 mmol, 1.5 equiv) was added dropwise to an orange solution of **1** (1.63 g, 2.56 mmol) in diethyl ether (40 mL) at ca. –10 °C. The solution initially became a green color, but it had changed to yellow-orange after the addition of the MeLi was completed. The solution was warmed to ca. 10 °C and stirred for 5 min, after which the solvent was removed under reduced pressure. The orange solid was extracted with hexanes (40 mL) and filtered through a Celite pad. The volume of the solution was reduced to ca. 3 mL under reduced pressure, and the flask was stored at ca. –20 °C for 2 days to afford orange-yellow crystals of **3** (1.51 g, 1.17 mmol, 91%). Mp = 166 °C (dec to brown). Anal. Calcd for C₇₅H₁₀₇LiSn: C, 71.89; H, 8.61. Found: C, 72.10; H, 9.05. UV–vis (hexanes) λ_{max}, ε (mol^{–1} cm^{–1}): 305 nm, 16050 (tails to 528 nm). ¹H NMR (C₆D₆, 399.77 MHz, 25 °C): δ –0.05 (s, 3 H, Sn(CH₃)₂), –0.01 (s, 3 H, Sn(CH₃)₂), 1.04–1.37 (m, 36 H, *o*- and *p*-CH(CH₃)₂), 2.77–3.00 (m, 8 H, *o*-CH(CH₃)₂), 3.10 (sept., 2 H, ³J = 6.8 Hz, *p*-CH(CH₃)₂), 3.54 (sept, 2 H, ³J = 7.0 Hz, *p*-CH(CH₃)₂), 6.92–7.40 (br m, 14 H, aromatic H's). ⁷Li {¹H} NMR (C₆D₆, 155.36 MHz): δ –3.35 (¹J(⁷Li–¹¹⁹Sn) = 736 Hz, ¹J(⁷Li–¹¹⁷Sn) = 702 Hz, ²J(⁷Li–¹¹⁹Sn) = 47 Hz). ¹³C {¹H} NMR (C₆D₆, 100.53 MHz): δ –3.82 (Sn–(CH₃)₂), –1.61 (Sn–(CH₃)₂), 23.01–24.12 (multiple peaks, *o*-CH(CH₃)₂), 25.58–26.18 (multiple peaks, *p*-CH(CH₃)₂), 29.95 (*o*-CH(CH₃)₂), 30.29 (*o*-CH(CH₃)₂), 30.94 (*o*-CH(CH₃)₂), 31.93 (*o*-CH(CH₃)₂), 34.27 (*p*-CH(CH₃)₂), 34.45 (*p*-CH(CH₃)₂), 120.08 (*m*-Trip), 120.20 (*m*-Trip), 120.65 (*m*-Trip), 120.83 (*m*-Trip), 121.01 (*m*-Trip), 121.19 (*m*-Trip), 121.25 (*m*-Trip), 121.32 (*m*-Trip), 130.00 (*m*-C₆H₃), 130.24 (*m*-C₆H₃), 125.47 (*p*-C₆H₃), 142.65 (*i*-Trip), 146.65 (*p*-Trip), 147.86 (*o*-Trip), 147.90 (*o*-Trip), 147.92 (*o*-Trip), 148.10 (*o*-Trip), 148.58 (*o*-C₆H₃), 148.72 (*o*-C₆H₃), 161.20 (*i*-C₆H₃). ¹¹⁹Sn {¹H} NMR (C₆D₆, 149.24 MHz): δ –431 (q, ¹J(¹¹⁹Sn–⁷Li) = 736 Hz, ¹J(¹¹⁹Sn–¹¹⁹Sn) = 4437 Hz, ¹J(¹¹⁹Sn–¹¹⁷Sn) = 4046 Hz), +151 (s, ¹J(¹¹⁹Sn–¹¹⁹Sn) = 4464 Hz, ¹J(¹¹⁹Sn–¹¹⁷Sn) = 4088 Hz) (²J(¹¹⁹Sn–⁷Li) = 47 Hz).

Sn(*t*-Bu)(C₆H₃-2,6-Trip₂) (4**).** *t*-BuLi (1.53 mL, 2.30 mmol, 1.1 equiv) was added dropwise to a pale yellow solution of **1** (1.33 g, 2.09 mmol) in hexanes (50 mL) at –78 °C. Slow warming to ca. –40 °C caused the solution to turn deep red, and by ca. –5 °C, the solution had turned dark purple. The solution was stirred at 25 °C for 1 h, and the solution was filtered through a Celite pad. The volume of the

Table 1. Selected Crystallographic Data for Compounds **2**·0.5 Hexane, **3**·0.5 Hexane, and **4**

	2 ·0.5 hexane	3 ·0.5 hexane	4
formula	C ₇₇ H ₁₁₁ Sn ₂	C ₇₈ H ₁₁₄ LiSn ₂	C ₄₀ H ₅₈ Sn
fw	1274.16	1296.13	657.55
crystal color/habit	green block	yellow block	purple-red shard
crystal system	monoclinic	triclinic	monoclinic
space group	<i>P</i> 2 ₁ / <i>n</i> (No. 14)	<i>P</i> 1 (No. 2)	<i>C</i> 2/ <i>c</i> (No. 15)
<i>a</i> (Å)	16.8704(5)	14.4163(6)	32.1821(13)
<i>b</i> (Å)	19.2696(6)	15.9717(7)	9.5744(4)
<i>c</i> (Å)	21.4850(6)	19.0328(8)	24.7577(10)
α (deg)		67.083(1)	
β (deg)	99.600(1)	74.633(1)	106.900(1)
γ (deg)		72.654(1)	
<i>V</i> (Å ³)	6886.7(4)	3797.2(3)	7299.0(5)
<i>Z</i>	4	2	8
ρ_{calcd} (mg/m ³)	1.229	1.134	1.197
μ (mm ⁻¹)	0.765	0.695	0.724
R1 ^a (obsd)	0.0383	0.0509	0.0385
wR2 (all data)	0.0957	0.1337	0.0865

$$^a \text{R1} = \sum ||F_o| - |F_c|| / |F_o|. \text{wR2} = [\sum w(F_o^2 - F_c^2)^2 / \sum w(F_o^2)]^{1/2}.$$

solution was reduced to ca. 2 mL, and the flask was stored at ca. -20 °C overnight, providing large, red-purple crystals of **4** (0.45 g, 0.68 mmol, 33%). Mp = 112–115 °C. Anal. Calcd for C₄₀H₅₈Sn₂: C, 73.06; H, 8.87. Found: C, 73.31; H, 8.73. UV-vis (hexanes) λ_{max} , ϵ (mol⁻¹ cm⁻¹): 485 nm, 655. ¹H NMR (C₆D₆, 399.77 MHz, 25 °C): 1.13 (d, 12 H, ³*J* = 7.2 Hz, *o*-CH(CH₃)₂), 1.17 (d, 12 H, ³*J* = 7.2 Hz, *o*-CH(CH₃)₂), 1.41 (d, 12 H, ³*J* = 7.2 Hz, *p*-CH(CH₃)₂), 1.35 (C(CH₃)₃), 2.75 (sept., 2 H, ³*J* = 7.2 Hz, *p*-CH(CH₃)₂), 3.29 (sept., 4 H, ³*J* = 7.2 Hz, *o*-CH(CH₃)₂), 7.05–7.25 (br m, 3 H, *p*- and *m*-C₆H₅), 7.34 (s, 4 H, *m*-Trip). ¹³C {¹H} NMR (C₆D₆, 100.53 MHz): δ 23.08 (*o*-CH(CH₃)₂), 24.21 (*p*-CH(CH₃)₂), 26.76 (*o*-CH(CH₃)₂), 27.55 (C(CH₃)₃), 31.02 (*o*-CH(CH₃)₂), 34.74 (*p*-CH(CH₃)₂), 70.07 (C(CH₃)₃), ¹*J*(¹³C–^{119/117}Sn) = 160 Hz), 121.51 (*m*-Trip), 126.72 (*p*-C₆H₅), 129.60 (*m*-C₆H₅), 135.18 (*i*-Trip), 144.62 (*p*-Trip), 147.02 (*o*-Trip), 149.08 (*o*-C₆H₅), 179.94 (*i*-C₆H₅), ¹*J*(¹³C–^{119/117}Sn) = 286/274 Hz. ¹¹⁹Sn {¹H} NMR (C₆D₆, 149.20 MHz): δ 1904.

X-ray Crystallographic Studies. The crystals were removed from the Schlenk tube under a stream of N₂ and immediately covered with a layer of hydrocarbon oil. A suitable crystal was selected, attached to a glass fiber, and immediately placed in a low-temperature nitrogen stream.⁷ All data were collected near 130 K using Bruker SMART 1000 (Mo K α radiation and a CCD area detector). The SHELXTL version 5.03 program package was used for the structure solutions and refinements.⁸ Absorption corrections were applied using the SADABS program.⁹ The crystal structures were solved by direct methods and refined by full-matrix least-squares procedures. All non-hydrogen atoms were refined anisotropically. Hydrogen atoms were included in the refinement at calculated positions using a riding model included in the SHELXTL program. Compounds **2** and **3** were crystallized from hexanes as the solvates **2**·0.5 hexane and **3**·0.5 hexane. The structure of **4** displays a partial occupancy by two species, the stannanediyl Sn-(*t*-Bu)C₆H₃-2,6-Trip₂ (**4**, 83% occupancy) and the isomeric stannanediyl Sn(*i*-Bu)C₆H₃-2,6-Trip₂ (17% occupancy) as a result of contamination of commercial *t*-BuLi solutions with *i*-BuLi. An anomalous electron density of 2.86 electrons/Å³ was observed within the covalent radius of Sn(2) in which is attributed to uncorrected absorption effects. Some details of the data collection and refinement are given in Table 1. Further details are provided in the Supporting Information.

Results and Discussion

Synthesis. The generation of compounds **2** and **3** can be accounted for in accordance with Scheme 1. Although the reaction of **1** with 1 equiv of MeLi, or preferably MeMgBr,

affords **2** in up to 85% yield, it is likely that Sn(Me)C₆H₃-2,6-Trip₂ is generated initially. However, this molecule apparently reacts rapidly with another 1 equiv of MeLi or MeMgBr to give **5** or its equivalent magnesium halide derivative. This species may then react further with **1** to afford the product **2**. In addition, compound **2** may be converted to **3** by its reaction with a further 1 equiv of LiMe. Alternatively, **3** can be generated directly from the reaction of **1** with 1.5 equiv of MeLi. In contrast to this reaction sequence, treatment of **1** with *t*-BuLi generates neutral Sn(*t*-Bu)C₆H₃-2,6-Trip₂, **4**, directly which, probably for steric reasons, does not react further with *t*-BuLi to generate a *t*-Bu-substituted analogue of **5**. Attempts to convert **2** into its symmetrical isomer **6** by a thermal rearrangement resulted in decomposition.

Since the overall steric congestion in **2** and the putative **6** should be similar, the preference for the symmetric structure **2** over its unsymmetric isomer **6** is unlikely to be due to steric effects. It is more probable that the instability of **6** is a result of the difference in the Sn–Sn bond strengths of the two compounds. Tetraorganoditin species such as **6** are often referred to as “distannenes” owing to their stoichiometric resemblance to their carbon analogues, the alkenes. But this name can be a misleading¹⁰ one since the currently known examples dissociate in solution owing to the weakness of the Sn–Sn bond. For example the Sn–Sn bond enthalpy¹¹ of {(Me₃Si)₂CH}₂SnSn-{CH(SiMe₃)₂}₂, which has the shortest Sn–Sn bond, 2.768(1) Å,^{4b} in “distannenes”, is 12.6 kcal mol⁻¹. This is much less than typical¹² Sn–Sn single bond enthalpies which are ca. 40 kcal mol⁻¹. Thus, it can be argued that, if **6** has a comparable (ca. 10 kcal mol⁻¹) Sn–Sn bond energy and it is to be energetically preferred over **2**, ca. 30 kcal mol⁻¹ would have to be found from the differences in tin carbon bond strengths in **2** and **6** to compensate for this difference. It seems doubtful that such differences in energy between tetravalent and divalent tin–carbon bonds would be sufficient to overcome this obstacle.¹³ In addition, it is notable that calculations¹⁴ on model hydrogen compounds of formula Sn₂H₄ indicate that the doubly bridged *trans*-HSn(μ -H)₂SnH is more stable than the unsymmetric stannylstannanediyl H₃Sn–SnH but that the latter is more stable than the “distannene” form H₂SnSnH₂. The lower bridging tendency of the methyl group suggests that the bridging structure in MeSn(μ -Me)₂SnMe may not be the most stable, and that the Me₃Sn–SnMe isomer may be the preferred one for the hypothetical species Sn₂Me₄ although this has not been substantiated by calculations. The high sensitivity¹⁰ of the “soft double bond”¹⁵ in distannenes to steric effects also suggests that dissociation to monomers would be preferred over rearrangement to the unsymmetrical isomer. In the previously known “distannenes” such a rearrangement would have resulted in three bulky groups at one tin atom which would be disfavored sterically. In **2**, however, such a configuration is feasible since two of these substituents are relatively small methyl groups.

- (10) Power, P. P. *Dalton Trans.* **1998**, 2939.
- (11) Zilm, K. W.; Lawless, G. A.; Merrill, R. M.; Millar, J. M.; Webb, G. G. *J. Am. Chem. Soc.* **1987**, *109*, 7236.
- (12) Simoes, J. A. M.; Liebman, J. F.; Slayden, S. W. Thermochemistry of Organometallic Compounds of Germanium, Tin and Lead. In *The Chemistry of Organic Germanium, Tin and Lead Compounds*; Patai, S., Ed.; Wiley: Chichester, 1995; Chapter 4.
- (13) Indeed there is evidence to suggest that some bonds to divalent tin (i.e., Sn(II)–N) are stronger than their Sn(IV)–N counterparts. See: Lappert, M. F.; Power, P. P.; Sanger, A. R.; Srivastava, R. C. *Metal and Metalloid Amides*; Ellis Horwood-Wiley: Chichester, 1979; p 265.
- (14) Trinquier, G. *J. Am. Chem. Soc.* **1991**, *113*, 144.
- (15) Driess, M.; Grützmacher, H. *Angew. Chem., Int. Ed. Engl.* **1996**, *35*, 828.

(7) Hope, H. *Prog. Inorg. Chem.* **1995**, *41*, 1.

(8) SHELXTL version 5.1: Bruker AXS, Madison, WI, 1998.

(9) SADABS, an empirical absorption correction program part of the SAINTPlus NT version 5.0 package, BRUKER AXS, Madison, WI, 1998.

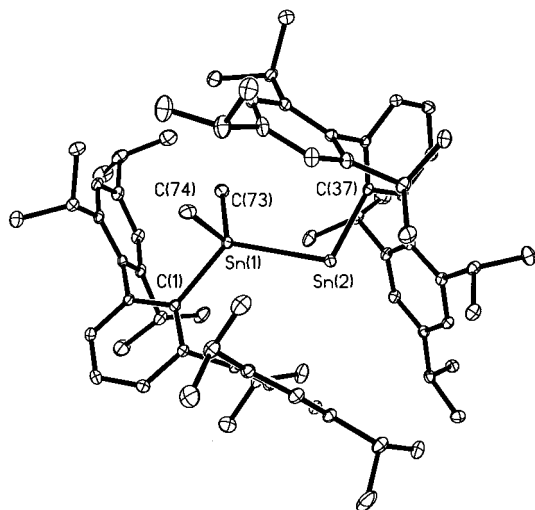


Figure 1. Thermal ellipsoid (30%) plot of **2**. H atoms are not shown. Selected bond distances and angles are given in Table 2.

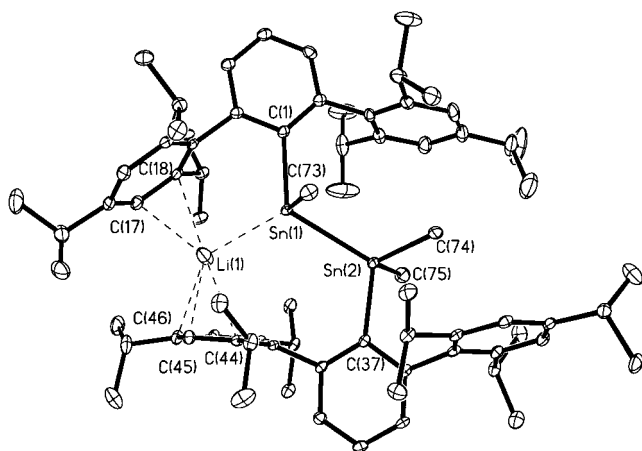


Figure 2. Thermal ellipsoid (30%) plot of **3**. H atoms are not shown. Selected bond distances and angles are given in Table 2.

Structural Data and Bonding. The structure of **2** is illustrated in Figure 1. It consists of well-separated molecules that crystallize along with 2.0 equiv of hexane per unit cell or 0.5 hexane per asymmetric unit. No strong interactions are apparent between the molecules themselves or with the co-crystallized hexane. It can be seen that the two tin centers are quite distinct since Sn(1) is bound to three carbons as well as Sn(2), whereas Sn(2) is two coordinate with bonds to Sn(1) and C(37). The geometry at Sn(1), whose interligand angles vary from 93.56(9) to 119.30(6)°, is grossly distorted from idealized tetrahedral. This can be attributed to the large variation in size and electronic properties of the substituent groups. The widest angle Sn(2)–Sn(1)–C(1) = 119.30(6)° involves the bulky aryl substituent. The Sn(1)–C bond lengths are in the range 2.164(2) to 2.201(2) Å with the latter value associated with the bulky aryl group. The two coordinate Sn(2) center has an interligand angle of 101.17(5)° as well as Sn(2)–C(37) and Sn(2)–Sn(1) bond lengths of 2.227(2) Å and 2.8909(2) Å. Previous results¹⁶ have shown that tin–carbon and tin–tin distances in catenated tin compounds are significantly affected by the steric properties of the organo groups. Comparison of

the Sn–C and Sn–Sn bond lengths in **2** with those observed in other sterically crowded molecules shows that they display some, but not an excessive, elongation. For instance, comparison of the Sn–C distances for the tin methyl groups in Me₃SnSnPh₃ (Sn–C(Me) = 2.138(5) Å),¹⁷ shows that they are ca. 0.03 Å shorter than the Sn–C(Me) bonds (ca. 2.17 Å) in **2**. However, in the more crowded molecule (t-Bu)₂TripSnSnTrip(t-Bu)₂,¹⁸ the Sn–C(t-Bu) bonds are significantly longer at ca. 2.26 Å. Similarly, the Sn(1)–C(1) distance, 2.201(2) Å, to the bulky terphenyl group is 0.06 Å longer than the Sn–C(Ph) distances in Ph₃SnSnPh₃,¹⁹ but is shorter than the Sn–C(Trip) bond of ca. 2.22 Å in (t-Bu)₂TripSnSnTrip(t-Bu)₂. The two-coordinate Sn(II) features a slightly longer Sn–C bond distance of 2.227(2) Å, but this is within the previously known range (2.21–2.23 Å) for two-coordinate Sn(II)-aryl derivatives.³

The most interesting structural parameters in **2** are the Sn(1)–Sn(2) bond distance, 2.8909(2) Å, and the interligand angle of 101.17(5)° at Sn(2). The only known structure with a bond between a divalent and tetravalent tin concerns Sn(2)–{(Me₃Si)₂CH}C₅H₄N{Sn(SiMe₃)₃},²⁰ which has an Sn–Sn bond 2.8689(5) Å long between four-coordinate and three-coordinate tin centers. The Sn–Sn distance in **2** is slightly longer despite the lower (two) coordination at one of its tin atoms. The slightly increased Sn–Sn distance is probably due to the large size of the terphenyl substituents. Nonetheless, the tin–tin bond cannot be regarded as being unduly lengthened since Sn–Sn bonds as long as 3.034(1) Å have been observed in previously mentioned (t-Bu)₂TripSnSnTrip(t-Bu)₂ compound.¹⁸ The interligand angle at Sn(2) is in the middle of the known range (87–118°)^{4,21} for divalent diorganotin(II) compounds, which also suggests a moderate degree of crowding in **2**.

The structure of **3** (Figure 2) has many similarities to that of **2**. In **3** both tins are four-coordinate, but Sn(1) has the same formal oxidation state (i.e., Sn(I)) as the two-coordinate tin center (i.e., Sn(2)) in **2**. Accordingly, the Sn–Sn bond length in **3**, 2.8508(4) Å, is similar to that in **2** although it displays some shortening. Possibly, the four-coordination in both tins leads to an increase s–p orbital mixing in the Sn–Sn bond which leads to the shorter Sn–Sn distance. However, the Sn(1)–C bond lengths, 2.202(4) Å (Me) and 2.259(4) Å (terphenyl), are slightly longer than those to Sn(2), perhaps as a result of the negative charge density at Sn(1) which reduces the ionic contribution to the Sn–C bond strengths. The Li–Sn(1) distance, 2.685(8) Å, is extremely short in comparison to the 2.871(7) Å observed in the complex [Li(PMDETA)SnPh₃],²² or the 2.89(4) Å in (THF)₃LiSn{N(SiMe₃)CH₂}₃CCCH₃.²³ It is possible that the simultaneous binding of the Li⁺ ion by the ortho-Trip groups of the terphenyls plays a role in the shortening of the distance. The Li–Sn bond is maintained in solution as shown by the observation of large ⁷Li–^{119/117}Sn couplings. The

(16) (a) Puff, H.; Breuer, B.; Gehrke-Brinkmann, G.; Kind, P.; Reuter, H.; Schuh, W.; Wald, W.; Weidenbruch, G. *J. Organomet. Chem.* **1989**, *363*, 265. (b) Schneider-Koglin, C.; Behrends, K.; Dräger, M. *J. Organomet. Chem.* **1993**, *448*, 29. (c) Sita, L. *Adv. Organomet. Chem.* **1995**, *38*, 189.

(17) Parkanyi, L.; Kalman, A.; Pannell, K. H.; Cervantes-Lee, F.; Kapoor, R. N. *Inorg. Chem.* **1996**, *35*, 6622.
 (18) Weidenbruch, M.; Schläefke, J.; Peters, K.; Schnering, H. G. v. *J. Organomet. Chem.* **1991**, *414*, 319.
 (19) (a) Preut, H.; Haupt, H.; Huber, H. Z. *Anorg. Allg. Chem.* **1973**, *396*, 81. (b) Piana, H.; Kirchgassner, W. S.; Schubert, U. *Chem. Ber.* **1991**, *124*, 743. (c) Eckardt, K.; Fuess, H.; Hattori, M.; Ikeda, R.; Ohki, H.; Weiss, A. Z. *Naturforsch A* **1995**, *50*, 758.
 (20) Cardin, C. J.; Cardin, D. J.; Constantine, S. P.; Todd, A. K.; Teat, S. T.; Coles, S. *Organometallics* **1998**, *17*, 2144.
 (21) (a) Weidenbruch, M. *Eur. J. Inorg. Chem.* **1999**, 373. (b) Power, P. P. *Chem. Rev.* **1999**, *99*, 3463.
 (22) Reed, D.; Stalke, D.; Wright, D. S. *Angew. Chem., Int. Ed. Engl.* **1991**, *30*, 1495.
 (23) Hillmann, K. W.; Gade, L. H.; Gevert, O.; Steinert, P.; Lauher, J. *Inorg. Chem.* **1995**, *34*, 4069.

Table 2. Selected Bond Lengths (Å) and Angles (°) for **2–4**

2			
Sn(1)–Sn(2)			2.8909(2)
Sn(1)–C(1)			2.201(2)
Sn(1)–C(73)			2.164(2)
Sn(1)–C(74)			2.182(3)
Sn(2)–C(37)			2.227(2)
Sn(2)–Sn(1)–C(1)			119.30(6)
Sn(1)–Sn(2)–C(37)			101.17(5)
C(1)–Sn(1)–C(73)			112.74(9)
C(1)–Sn(1)–C(74)			93.56(9)
C(73)–Sn(1)–C(74)			109.37(10)
C(73)–Sn(1)–Sn(2)			115.67(7)
C(74)–Sn(1)–Sn(2)			102.58(6)
C(6)–C(1)–Sn(1)			118.3(2)
C(2)–C(1)–Sn(1)			122.02(15)
C(38)–C(37)–Sn(2)			117.06(15)
C(42)–C(37)–Sn(2)			123.32(15)
3			
Sn(1)–Sn(2)	2.8508(4)	Li–C(17)	2.538(9)
Sn(1)–C(1)	2.259(4)	Li–C(18)	2.601(9)
Sn(1)–C(73)	2.202(4)	Li–C(44)	2.707(9)
Sn(1)–Li	2.685(8)	Li–C(45)	2.367(9)
Sn(2)–C(37)	2.229(4)	Li–C(46)	2.513(9)
Sn(2)–C(74)	2.159(4)	Li-centroid (C13–C18)	2.746
Sn(2)–C(75)	2.172(4)	Li-centroid (C43–C48)	2.424
C(1)–Sn(1)–Sn(2)	120.06(9)		
C(37)–Sn(2)–Sn(1)	110.81(9)		
C(1)–Sn(1)–C(73)	95.02(14)		
C(1)–Sn(1)–Li	110.9(2)		
C(73)–Sn(1)–Sn(2)	90.05(12)		
C(73)–Sn(1)–Li	121.1(2)		
C(37)–Sn(2)–C(74)	108.14(14)		
C(37)–Sn(2)–C(75)	96.71(15)		
C(74)–Sn(2)–C(75)	102.78(18)		
C(2)–C(1)–Sn(1)	112.8(2)		
C(6)–C(1)–Sn(1)	130.5(3)		
C(38)–C(37)–Sn(2)	121.3(3)		
C(42)–C(37)–Sn(2)	121.8(2)		
Li–Sn(1)–Sn(2)	116.7(2)		
C(74)–Sn(2)–Sn(1)	111.33(12)		
C(75)–Sn(2)–Sn(1)	125.33(12)		
4			
Sn(1)–C(1)			2.2114(18)
Sn(1)–C(37)			2.227(2)
C(1)–Sn–C(37)			101.61(8)
C(2)–C(1)–Sn			121.03(13)
C(6)–C(1)–Sn			118.76(13)

Sn(2)–C bond lengths are slightly longer than the corresponding distances in **2**.

The monomeric, two-coordinate tin(II) alkyl/aryl **4** (Figure 3) has the expected V-shaped coordination at tin and is isomorphous with its lead analogue.¹ The Sn–C(*t*-Bu) distance 2.227(2) Å is marginally longer than the 2.211(2) Å Sn–C(terphenyl) bond length. The latter is virtually identical to the 2.213(13) Å Sn–C bond previously reported for the iodide Sn(I)C₆H₃-2,6-Trip₂.²⁴ The C–Sn–C angle, 101.61(6)°, is slightly wider than the 100.5(5)° in its lead analogue, and it is very similar to the 102.6(3)° observed for the C–Sn–I angle in Sn(I)C₆H₃-2,6-Trip₂ and the 101.17(5)° angle at Sn(2) in **2**. As already discussed for **2**, these angles are near the middle of the range for two-coordinate diorganotin species.

NMR Spectroscopy. The solution ¹¹⁹Sn NMR spectra for compounds **2–4** provide considerable information on the structural and electronic environment at tin. The ¹¹⁹Sn NMR spectra of compounds **2** and **4** were also studied in more detail by CP MAS ¹¹⁹Sn NMR spectroscopy, but this information will

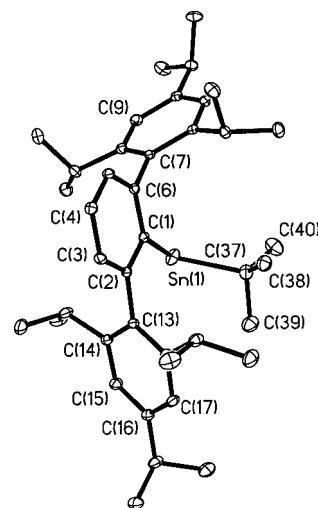


Figure 3. Thermal ellipsoid (30%) plot of **4**. H atoms are not shown. Selected bond distances and angles are given in Table 2.

be discussed elsewhere.²⁵ In general, the ¹¹⁹Sn NMR chemical shifts of divalent tin species (>+200 ppm) lie considerably downfield of their tetravalent (<+200 ppm) counterparts.²⁶ The ¹¹⁹Sn NMR chemical shift of compound **4** (δ 1904) is consistent with this generalization and is indicative of the deshielded environment at the tin atom as a result of its lower coordination number. The chemical shift of the divalent tin in **2** is 2856.9 ppm which is further downfield than the shifts observed for **4**, Sn[C₆H₂-2,4,6-{CH(SiMe₃)₂}₃] (δ = 2208),^{3b}

SnC(SiMe₃)₂(CH₂)₂C(SiMe₃)₂ (δ = 2323)^{3a} or Sn{CH(SiMe₃)₂}₂ (δ = 2315).¹⁰ The downfield shift is probably due to an increase in paramagnetic effects as a result of the substitution of an organic group by the more electropositive -Sn(Me)₂C₆H₃-2,6-Trip₂ moiety. The ¹¹⁹Sn NMR chemical shift of the tetravalent site in **2** is +257.4 ppm, which is at the lower end of the range normally found for four-coordinate tin compounds.²⁶ The value of the coupling constant (^{119/117}Sn–^{119/117}Sn) between the tin atoms in compound **2** is 8330 Hz, which is larger than is normally observed for hexaorganotin species such as Ph₃–SnSnPh₃ (¹J(¹¹⁷Sn–¹¹⁹Sn) = 4470 Hz).²⁶ It is also greater than the coupling in the four-coordinate tin/three-coordinate tin species reported by Cardin and co-workers¹⁶ by ca. 2000 Hz. The tin–tin coupling constants observed in **3** (¹J(^{117/119}Sn–^{117/119}Sn) = ca. 4050 Hz) is very close to the value in **2**. In **3** the coordination number of the Sn(I) center is increased from 2 to 4, and this results in a dramatic upfield change in the ¹¹⁹Sn chemical shift by ca. 3300 ppm to –431 ppm. The shift of the four-coordinate tin atom is moved by only ca. 100 ppm downfield. The assignment of the two resonances in the ¹¹⁹Sn NMR spectrum of **3** is also facilitated by the observation of coupling to ⁷Li (*I* = 3/2). The resonance at –431 ppm is split into a quartet with large ¹J(¹¹⁹Sn–⁷Li) coupling of ca. 740 Hz. The other tin resonance at +151 ppm has a much smaller coupling of 47 Hz (²J = ¹¹⁹Sn–⁷Li). The coupling of 740 Hz is the largest one bond ¹¹⁹Sn–⁷Li coupling observed to date,²⁷ which is consistent with the short Sn–Li distance observed in the X-ray crystal structure.

The ¹H and ¹³C NMR spectra of **2** indicate that the Trip groups are rotationally hindered. Broad singlets in the ¹H NMR

(25) Eichler, B. E.; Phillips, B. L.; Power, P. P.; Augustine, M. P. *Inorg. Chem.* **2000**, *39*, 5450.

(26) Wrackmeyer, B. *Annu. Rep. NMR Spectrosc.* **1999**, *38*, 203.

(27) Wrackmeyer, B. *Annu. Rep. NMR Spectrosc.* **1985**, *16*, 73.

(24) Pu, L.; Olmstead, M. M.; Power, P. P.; Schiemenz, B. *Organometallics* **1998**, *17*, 5602.

spectrum at ca. 3 ppm appear in the region of the methine hydrogens ($CH(CH_3)_2$) of the isopropyl groups. The ^{13}C NMR spectrum of the *o*-isopropyl groups also displays two sets of resonances. The two tin methyl groups are assignable to a singlet at -0.34 ppm in the 1H spectrum and a broad singlet at $+0.34$ ppm in the ^{13}C spectrum. The 1H and ^{13}C NMR spectra of **3** are more complex than those of **2**. Not only are the two 2,6-Trip $_2C_6H_3^-$ groups inequivalent owing to the different ligand sets at the tins (i.e., $-Me_2Sn-SnMeLi-$), in addition, one Trip group on each terphenyl ligand is coordinated to a lithium ion (see Figure 2). Thus, all four Trip groups in the molecule are inequivalent. Two singlets are observable for the methyl groups on tin in both the 1H and ^{13}C NMR spectra of **3**. The methyl group bound to the same tin as the lithium atom may couple to 7Li , thereby reducing the height of the peaks and possibly rendering it unobservable above the baseline.

Conclusion. The unsymmetric stannanestannanediyl **2** is preferred over the symmetric isomer **6** owing to the weakness of the Sn–Sn polar dative bonds in **6** relative to the covalent Sn–Sn single bond in **2**. The isolation of **2** is made possible by the unique steric combination of the large terphenyl ligands and the small methyl groups which, unlike other large substituents, stabilize the bonding between two and four coordinate tins.

Acknowledgment. We are grateful to the National Science Foundation for financial support.

Supporting Information Available: Three X-ray files, in CIF format, are available. This material is available free of charge via the Internet at <http://pubs.acs.org>.

IC0005137